

CHEMISTRY

AN **ASIAN** JOURNAL

www.chemasianj.org

Accepted Article

Title: Alcohol-soluble Electron Transport Materials for Fully Solution-processed Green PhOLEDs

Authors: Fudong Chen, Shirong Wang, Yin Xiao, Feng Peng, Nonglin Zhou, Lei Ying, and Xiangao Li

This manuscript has been accepted after peer review and appears as an Accepted Article online prior to editing, proofing, and formal publication of the final Version of Record (VoR). This work is currently citable by using the Digital Object Identifier (DOI) given below. The VoR will be published online in Early View as soon as possible and may be different to this Accepted Article as a result of editing. Readers should obtain the VoR from the journal website shown below when it is published to ensure accuracy of information. The authors are responsible for the content of this Accepted Article.

To be cited as: *Chem. Asian J.* 10.1002/asia.201800320

Link to VoR: <http://dx.doi.org/10.1002/asia.201800320>

A Journal of



A sister journal of *Angewandte Chemie*
and *Chemistry – A European Journal*

WILEY-VCH

Alcohol-soluble Electron Transport Materials for Fully Solution-processed Green PhOLEDs

Fudong Chen,^[a,b] Shirong Wang,^[a,b] Yin Xiao,^[a,b] Feng Peng,^[c] Nonglin Zhou^[a,b], Lei Ying^{*[c]} and Xianggao Li^{*[a,b]}

[a] *Tianjin University, School of Chemical Engineering and Technology, Tianjin China*

[b] *Collaborative Innovation Center of Chemical Science and Engineering, Tianjin 300072, China*

[c] *Institute of Polymer Optoelectronic Materials and Devices, State Key Laboratory of Luminescent Materials and Devices, South China University of Technology, Guangzhou 510640, P. R. China.*

*Corresponding author. *Email address:* lixianggao@tju.edu.cn (Xianggao Li); msleiyang@scut.edu.cn (Lei Ying)

Accepted Manuscript

Abstract: Two alcohol-soluble electron transport materials (ETMs), diphenyl(4-(1-phenyl-1*H*-benzo[*d*]imidazol-2-yl)phenyl)phosphine oxide (pPBIPO) and (3,5-bis(1-phenyl-1*H*-benzo[*d*]imidazol-2-yl)phenyl)diphenylphosphine oxide (mBPBIPO), are synthesized. Physical properties of the two ETMs are investigated, which show high electron transport mobilities of $1.67 \times 10^{-4} \text{ cm}^2 \text{ V}^{-1} \text{ s}^{-1}$ and $2.15 \times 10^{-4} \text{ cm}^2 \text{ V}^{-1} \text{ s}^{-1}$, high glass transition temperatures of 81 °C and 110 °C and deep LUMO energy levels of -2.87 eV and -2.82 eV, respectively. The solubility of PBIPO in *n*-butyl alcohol is more than 20 mg mL⁻¹, which can meet the requirement of the fully solution-processed organic light emitting diodes (OLEDs). Basted on it, fully solution-processed green phosphorescent OLEDs using alcohol-soluble PBIPO as ETLs are fabricated, which exhibit high efficiencies (current efficiency, power efficiency, external quantum efficiency) of 38.43 cd A⁻¹, 26.64 lm W⁻¹ and 10.87%. Compared with devices without PBIPO as ETMs, performance of these devices is significantly increased, which indicates the excellent electron transport properties of PBIPO.

Introduction

In the recent years, organic light emitting diodes (OLEDs) have attracted intense attention owing to their potential application in display panels, solid-state lighting sources and flexible displays ^[1]. Although highly efficient OLEDs are still mainly produced by evaporation methods, solution-processed method is more suitable for flexible devices and large-size flat-panel displays ^[2]. However, the most serious problem of solution-processed method is that the lower layer will be redissolved and affected by the solvent used of the upper layer, leading to poor performance of these devices^[2b]. One approach to overcome this problem is to utilize orthogonal solvents^[3] in the spin-coating process, which need water soluble hole transport materials (HTMs), oil soluble emitting layer (EML) and alcohol soluble electron transport materials (ETMs). The first two materials above such as PEDOT: PSS ^[4] and Ir complex^[5] have been developed, so alcohol soluble ETMs is urgent needed for solution-processed OLEDs.

Solution-processed OLEDs have been fabricated using alcohol soluble polyelectrolytes as ETMs ^[4c, 6].

However, it has been demonstrated that the ionic side group attachment to the polymer side chains may lead to the unanticipated electrochemical doping effect [7]. The synthesis and purification of small molecule alcohol soluble ETMs can be more convenient compared to the polyelectrolytes, which is more suitable for solution-processed OLEDs [2]. In order to improve the alcohol solubility of the small molecule ETM, it is necessary to modify the ETM with strong electron-withdrawing groups, such as the diphenyl-phosphine oxide (PO) group [3a, 8]. PO group has merits as follows: 1) PO group is widely used as electron-withdrawing unit to achieve high electron transport mobility, producing excellent ETMs [2b, 9]. 2) According to the theory of similar dissolve mutually, the introduction of the polar phosphine oxide moiety can afford higher solubility in polar solvents, such as methanol, 2-propanol and n-butyl alcohol.

Using alcohol soluble ETMs modified with PO to fabricate fully solution-processed OLEDs has been reported. For example, in 2014, Wei Jiang et al. designed the novel alcohol soluble ETM, tris(4-(diphenylphosphoryl)phenyl)benzene, for fully solution-processed white phosphorescent OLED (WPhOLED), exhibiting a high current efficiency (CE) of 32.6 cd A⁻¹ [2b]. In 2015, Ronghua Liu et al. designed the alcohol soluble ETM, ((1,3,4-oxadiazole-2,5-diyl)bis(4,1-phenylene))bis(diphenylphosphine oxide), and fully solution-processed WPhOLED were fabricated with a high CE_{max} of 18.96 cd A⁻¹ [2a]. In 2016, Xinxin Ban et al. designed 1,3,5-tris(diphenylphosphoryl)benzene (TPO) with high triplet energy level (T₁) and fully solution processed WPhOLED with CE_{max} of 38.5 cd A⁻¹ and power efficiency (PE) of 22.5 lm W⁻¹ were fabricated utilizing TPO as exciplex-type host materials [4a].

With good electron transport properties and deep LUMO levels, benzimidazole units are widely used as ETMs in OLEDs.[10] In particular, 1,3,5-tris(*N*-phenylbenzimidazol-2-yl)benzene (TPBI) has been used as ETM for OLEDs. Using TPBI as ETMs in phosphorescent OLED (PhOLEDs), external quantum efficiency (EQE) of 10.4 % has been obtained at much lower voltages compared to those without TPBI.[11] Additionally, TPBI exhibits

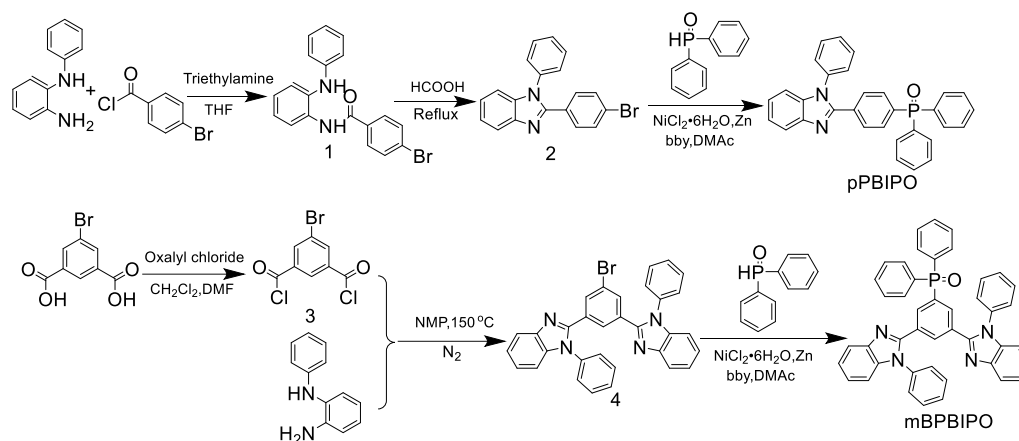
good hole-block properties owing to its high ionization potential.^[12] Inspired by the excellent properties of PO and benzimidazole, connecting PO with benzimidazole may result in high-performing ETMs with high electron mobility and high triplet energy level.

Herein, alcohol soluble ETMs, diphenyl(4-(1-phenyl-1*H*-benzo[*d*]imidazol-2-yl)phenyl)phosphine oxide (pPBIPO) and (3,5-bis(1-phenyl-1*H*-benzo[*d*]imidazol-2-yl)phenyl)diphenylphosphine oxide (mBPBIPO) were synthesized by attaching the PO group to the benzimidazole core. Their physical properties were investigated and fully solution-processed green PhOLEDs were fabricated. Efficiencies (CE, PE, EQE) of 38.43 cd A⁻¹, 26.64 lm W⁻¹, 10.87% were obtained utilizing mBPBIPO as ETL. Compared with devices without PBIPO as ETMs, efficiencies of these PhOLEDs were significantly increased by 1-2 folds and turn on voltages (V_{on}) were reduced after introducing PBIPO into devices, indicating the excellent electron transport properties of PBIPO.

Result and Discussion

Synthesis Routes

The synthesis procedure of diphenyl(4-(1-phenyl-1*H*-benzo[*d*]imidazol-2-yl)phenyl)phosphine oxide (pPBIPO) and (3,5-bis(1-phenyl-1*H*-benzo[*d*]imidazol-2-yl)phenyl)diphenylphosphine oxide (mBPBIPO) was illustrated in Scheme 1. Firstly, amide was synthesized by chloride according to the literature ^[13]. Then benzimidazole was synthesized by a cyclization reaction ^[13-14]. Finally, PBIPO was synthesized by a coupling reaction ^[14]. All compounds were characterized by ¹HNMR and HRMS (See ESI S1-S3).



Scheme 1. Molecular structure and synthetic routes of pPBIPO and mBPBIPO.

Photophysical properties

Figure 1a shows the UV-vis absorption and PL emission of the two compounds in CH_2Cl_2 . The two compounds exhibit very similar absorption and emission spectra profiles. The absorption spectra of pPBIPO and mBPBIPO show peaks at 232 nm, 301 nm and 233 nm, 308 nm in CH_2Cl_2 , respectively. The maximum absorption (λ_{abs}) at 301 nm and 308 nm may be attributed to the benzimidazole-centered $n-\pi^*$ transition^[15]. The energy gap (E_g) values of the two materials are 3.54 eV and 3.59 eV, respectively, which are calculated from the onset of the UV-vis absorption spectra. The maximum PL emission peaks of pPBIPO and mBPBIPO are 376 nm and 371 nm, respectively. The slight blue-shifted (5 nm) in the PL spectrum of mBPBIPO compared with that of pPBIPO may be attributed to the weak molecule interaction of mBPBIPO due to its larger steric hindrance and severed molecule distortion^[15-16].

In addition, as shown in Figure 1b, the T_1 levels of pPBIPO and mBPBIPO have been determined by the highest energy vibronic subband of the phosphorescence spectra at 77 K, which is 2.63 eV and 2.67 eV, respectively. The high triplet energy levels of pPBIPO and mBPBIPO can efficiently confine the emitting materials triplet excitons in the EML and improve charge recombination in the devices^[2b, 15].

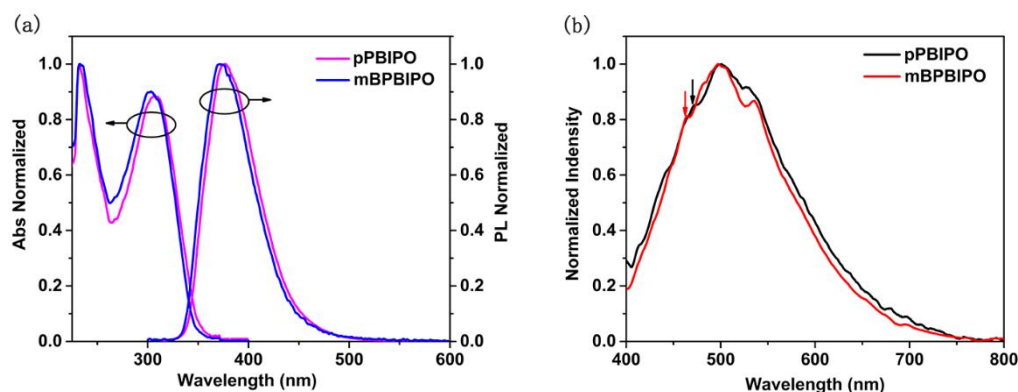


Figure 1. (a) UV-Vis absorption and PL spectra of pPBIPO and mBPBIPO. (b) Phosphorescence spectra of pPBIPO and mBPBIPO measured at 77K.

Electrochemical properties

Energy levels matching of semiconductors used in OLEDs are crucial to making high performance devices. Cyclic voltammetry (CV) of the two compounds, pPBIPO and mBPBIPO, was performed using Ag/AgNO₃ as the reference electrode to investigate their energy levels (See ESI Figure S4). Anhydrous tetrabutylammonium hexafluorophosphate (Bu₄NPF₆) was used as the supporting electrolyte in nitrogen-saturated CH₂Cl₂ solvent. The LUMO energy levels of pPBIPO and mBPBIPO were calculated to be -2.87 eV and -2.82 eV from the onset reduction potential using Fc/Fc⁺ as an internal standard.^[17] HOMO levels were nearly -6.41 eV for both compounds according to the LUMO levels and E_g obtained from the UV-vis absorption spectra.^[18] The nearly HOMO and LUMO levels may be attributed to the similar molecule structure.

Thermal properties and morphology

The thermal properties of the PBIPO were investigated through thermogravimetric analysis (TGA) and differential scanning calorimetry (DSC) in a nitrogen atmosphere (Figure 2a-2b). The glass transition temperatures (T_g) of pPBIPO and mBPBIPO are 81 °C and 110 °C and the decomposition temperatures (T_d) of pPBIPO and mBPBIPO are 371 °C and 355 °C, respectively. The lower T_d of mBPBIPO compared with pPBIPO may be attributed to the weak molecule rigidity due to its large steric hindrance and severed molecule distortion^[19]. The excellent thermal stabilities are quite significant for organic optoelectronic materials under spin-

coating process.^[20]

The power X-ray diffraction (XRD) spectra were measured to research the crystallization property and stability of the spin-coating PBIPO film (Figure 2c-2d). No matter before annealing or after annealing, the films show featureless peaks compared with glass substrate, implying that pPBIPPO and mBPBIPPO could form amorphous film by spin-coating process.^[21] What's more, atomic force microscopy (AFM) was used to investigate the surface morphology of PBIPPO spin-coating films (See ESI Figure S6). The root-mean-square (RMS) values of pPBIPPO and mBPBIPPO spin-coating films were 2.399 nm and 2.229 nm, respectively, demonstrating the formation of homogeneously films.

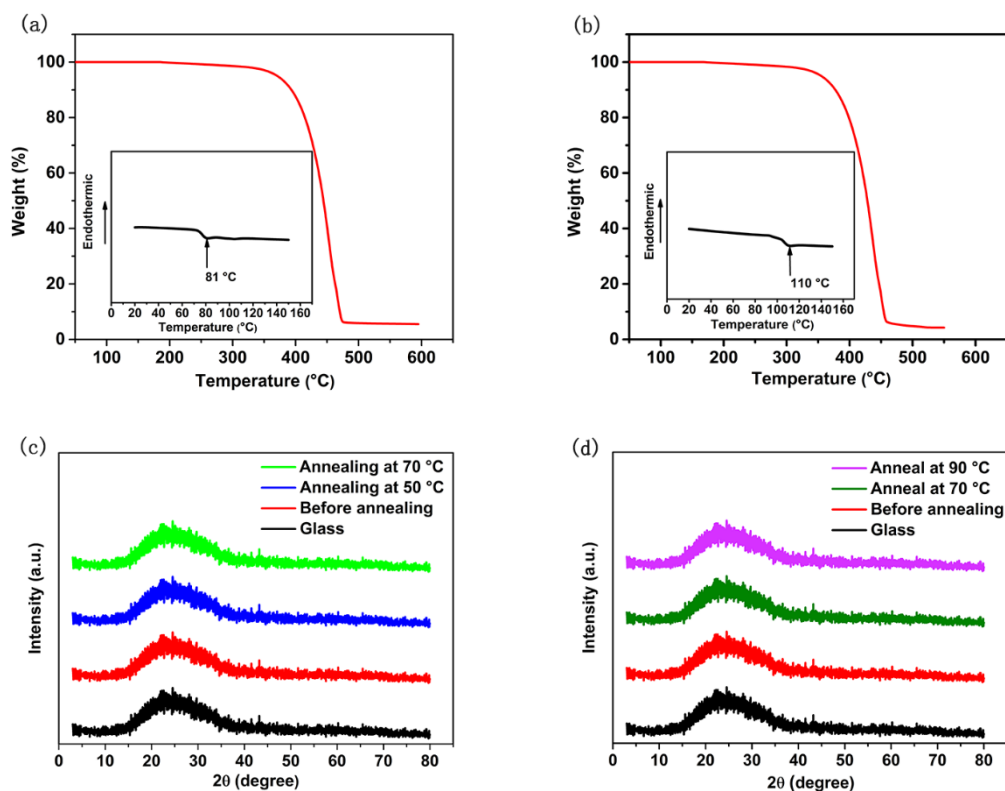


Figure 2. (a) TGA and DSC (Inset) thermograms of pPBIPPO. (b) TGA and DSC (Inset) thermograms of mBPBIPPO. (c) X-ray diffraction spectra of glass substrate and pPBIPPO spin-coating film on glass substrate. (d) X-ray diffraction spectra of glass substrate and mBPBIPPO spin-coating film on glass substrate.

Electron transport properties

Electron transport mobility (μ_e) is one of the most important parameter for electron transport materials.

Space-charge-limited current (SCLC) measurement was applied to evaluate μ_e of PBIPPO^[22]. The electron-only

devices were designed and fabricated with the construction of ITO/LiF (1 nm)/TPBI (10 nm)/PBIPPO (120 nm)/LiF (1 nm)/Al (120 nm), in which the LiF/Al layer served as the electron-injecting layer to ensure the ohmic contact required for SCLC method, while the LiF/TPBI layer near ITO were used as hole-block layer to ensure the single carrier device. According to the Mott-Gurney law:

$$J = \frac{9}{8} \mu_0 \varepsilon_0 \varepsilon_r \frac{E^2}{L} \exp(\gamma \sqrt{E})$$

where J is the measured current density, μ_0 is zero-field carrier mobility, ε_0 is the vacuum permittivity ($\varepsilon_0 = 8.85 \times 10^{-14} \text{ CV}^{-1} \text{ cm}^{-1}$), ε_r is the relative dielectric constant, E is the electron field, L is the thickness of the organic layer, γ is the field-activation factor. Accordingly, the μ_0 of pPBIPPO and mBPBIPPO can be estimated as $1.67 \times 10^{-4} \text{ cm}^2 \text{ V}^{-1} \text{ s}^{-1}$ and $2.15 \times 10^{-4} \text{ cm}^2 \text{ V}^{-1} \text{ s}^{-1}$, respectively (See Figure 3 or ESI Figure S5). The zero-field carrier mobility of mBPBIPPO is higher than that of pPBIPPO because mBPBIPPO molecule have two benzimidazole moiety, providing two sites for electron transportation. The high μ_0 of pPBIPPO and mBPBIPPO can match the hole transport mobility of HTM, which is beneficial to the balance of hole-electron carrier of devices.^[23]

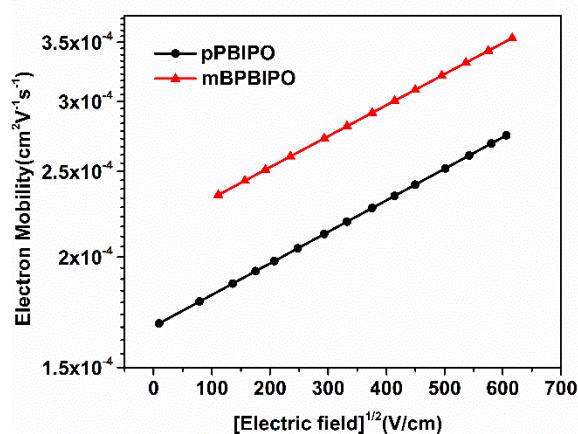


Figure 3. Dependence of electron mobilities of pPBIPPO and mBPBIPPO in electric field.

Alcohol Solubility

The alcohol solubility of ETM is of vital significance for the preparation of fully solution-processed OLEDs by orthogonal solvent methods. The solubility of PBIPPO in different alcohol was investigated and the detailed

dates are listed in Table 1. It is obvious that PBIPO has excellent methanol solubility, which is more than 500 mg mL⁻¹, and at the same time, its solubility in 2-propanol and n-butyl alcohol meets the requirement of fully solution-processed OLEDs. Considering the boiling point, viscosity and other parameters of the above three alcohol solvents, n-butyl alcohol solution of PBIPO was selected to fabricate the fully solution-processed OLEDs.

Table 1. Alcohol solubility of pPBIPPO and mBPBIPPO.

Compounds	methanol (mg mL ⁻¹)	2-propanol (mg mL ⁻¹)	n-butyl alcohol (mg mL ⁻¹)
pPBIPPO	>500	>20	>20
mBPBIPPO	>500	>20	>60

Electroluminescence properties

Emitting layer with good oil solubility and bad alcohol solubility is needed for fully solution-processed OLEDs. Herein, host 2: IrG1=95:5 were selected as an emitting layer (EML), in which host 2 and IrG1 was the host and guest green material respectively. The energy levels and chemical structures of materials used in devices were shown in Figure 4-5. First of all, we fabricated Device A as a control with the construction of ITO/PEDOT:PSS(40 nm)/host2:IrG1=95:5(65 nm)/CsF(0.8 nm)/Al(100 nm), in which ITO/PEDOT:PSS served as anode, host2:IrG1=95:5 served as the green phosphorescence EML, CsF/Al served as cathode and no ETL was utilized. Due to the lack of ETL, which results in the high energy level barriers and the unbalance of hole and electron, the two devices exhibited high V_{on} of 4.8 V and low efficiency (CE_{max} , PE_{max} , EQE_{max}) of 16.80 cd A⁻¹, 6.67 lm W⁻¹ and 4.73%. Then, in order to make sure that the n-butyl alcohol used in ETL preparation process would not affect the emitting layer prepared before, Device B was fabricated based on Device A with the construction of ITO/PEDOT:PSS(40 nm)/host2:Ir-G1=95:5(65 nm)/n-butyl alcohol(40 μ L)/CsF(0.8 nm)/Al(100 nm) by washing the emitting layer with 40 μ L n-butyl alcohol. Efficiency (CE_{max} , PE_{max} , EQE_{max}) of Device B only showed small drop of 15.24 cd A⁻¹, 5.99 lm W⁻¹ and 4.34% compared with that of Device A, which indicated that the emitting layer was almost unaffected by n-butyl alcohol used in ETL preparation process. EL spectra, current density-

voltage-luminance (J-V-L) curves, current efficiency-luminance-power efficiency (CE-L-PE), external quantum efficiency-luminance (EQE-L) curves were shown in Figure 6 and the detailed device parameters were summarized in Table 2.

Based on it, Device C and D, with pPBIPO (Device C) and mBPBIPO (Device D) as ETLs, were fabricated with the construction as follows: ITO/PEDOT:PSS(40 nm)/host2:IrG1=95:5(65 nm)/PBIPO(15 nm)/CsF(0.8 nm)/Al(100 nm). EL spectra, J-V-L curves, CE-L-PE, EQE-L curves were shown in Figure 6 and the device parameters were listed in Table 2. After introducing PBIPO into devices, the hole and electron were much balanced and the exciton was confined within the EML due to the high μ_e and high T_1 level of PBIPO. Much better device performance were obtained. The maximum luminance (L_{\max}) as high as 21441 cd m^{-2} and 39132 cd m^{-2} of Device C and D were observed while that of Device A was just 15521 cd m^{-2} . And V_{on} of Device C and D was reduced to 4.0 V compared with that of 4.8 V for Device A. What's more, pPBIPO (or mBPBIPO) endowed their Device C (or D) with efficiencies (CE, PE, EQE) up to 25.50 cd A^{-1} (25.00 cd A^{-1}), 11.37 lm W^{-1} (11.95 lm W^{-1}) and 7.20% (7.08%). Compared with Device A without PBIPO as ETL, L_{\max} of Device C and D were increased by 38% and 152%, CE_{\max} of Device C and D were increased by 52%.

In order to reduce the V_{on} and improve the device efficiency, PVK was introduced to further reduce the energy level barriers and block the triplet exciton in the ETM. Device E and F, with pPBIPO (Device E) and mBPBIPO (Device F) as ETLs, were fabricated with the construction of ITO/PEDOT:PSS(40 nm)/PVK(20 nm)/host2: IrG1=95:5(65 nm)/PBIPO(15 nm)/CsF(0.8 nm)/Al(100 nm). EL spectra, J-V-L curves, CE-L-PE, EQE-L curves were shown in Figure 6 and the device parameters were listed in Table 2. Obviously, efficiencies (CE_{\max} , PE_{\max} , EQE_{\max}) of Device E and F were increased highly. For Device F, high efficiencies (CE_{\max} , PE_{\max} , EQE_{\max}) of 38.43 cd A^{-1} , 26.64 lm W^{-1} , 10.87% and low V_{on} of 2.9 V were observed. Compared with Device C and D, efficiencies (CE_{\max} , PE_{\max} , EQE_{\max}) of Device E and F were highly raised by 26%, 43%, 26% and 54%, 123%,

54%, respectively. Because the photoluminescence quantum efficiency (PLQE) of the ETM prepared on the PVK layer (0.640) was higher than that observed on PEDOT:PSS (0.366), the PVK layer worked as an efficient exciton-block layer. The much higher device efficiency obtained after PVK was introduced arose from the much efficient hole injection and triplet exciton block effect.^[24] However, the L_{\max} of Device E and F were reduced, which can be attributed to the much lower current density due to the much higher resistance after introducing the PVK layer^[25]. In addition, one phenomenon should be noted, which is that the performance of devices used mBPBIPO as ETLs is much better than that of pBPBIPO after introducing PVK into devices as HTL. This phenomenon can be ascribed to the much higher μ_e of mBPBIPO than pBPBIPO, which can be more matchable with the hole transport mobility of PVK, leading to much better carrier balance of devices.

Generally, although fully solution-processed has the advantage of low-cost and material saving, devices fabricated by vacuum evaporation would exhibit much better performance due to the homogeneity of the thin film. Herein, Device G utilizing TPBI, whose molecular structure is similar with mBPBIPO, as ETM was fabricated with the construction of ITO/PEDOT:PSS(40 nm)/PVK(20nm)/host2: IrG1=95:5(65 nm)/TPBI(15 nm)/CsF(0.8 nm)/Al(100 nm) , in which TPBI was deposited by vacuum evaporation. EL spectra, J-V-L curves, CE-L-PE, EQE-L curves were shown in Figure 6 and the device parameters were listed in Table 2. Results indicated that Device G exhibited poorer performance, including high turn-on voltages (4.6 V), severer rolls-off, lower efficiency (34.75 cd A⁻¹, 21.14 lm W⁻¹, 8.48%) and lower luminance (8037cd m⁻²), compared with Device E and F, especially Device F. These results demonstrated the much better properties of the spin-coating mBPBIPO film than deposited TPBI film.

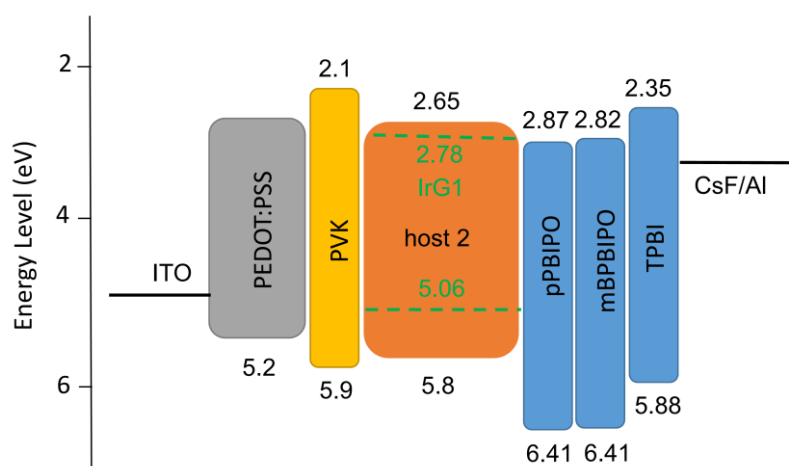


Figure 4. The energy level diagram of Device A-G.

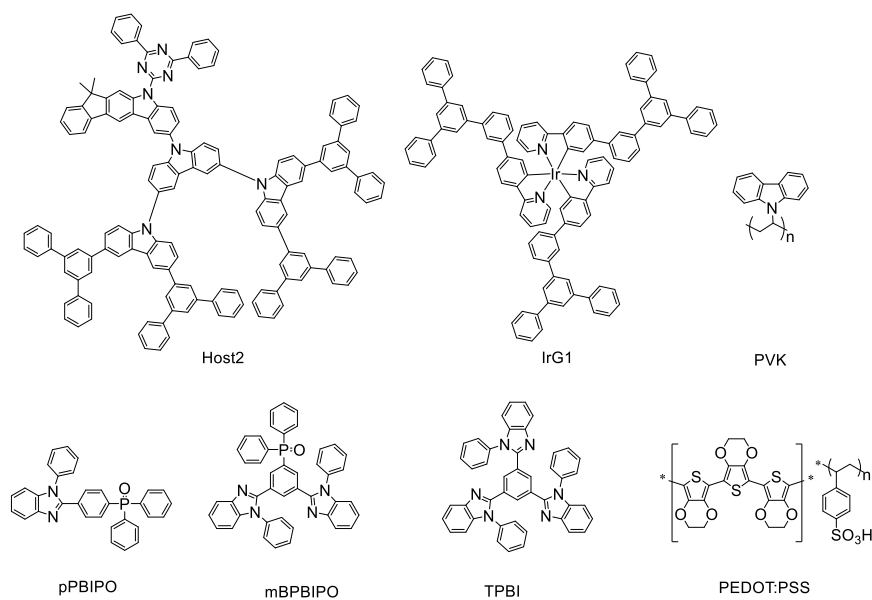


Figure 5. Molecular structure of materials used in devices

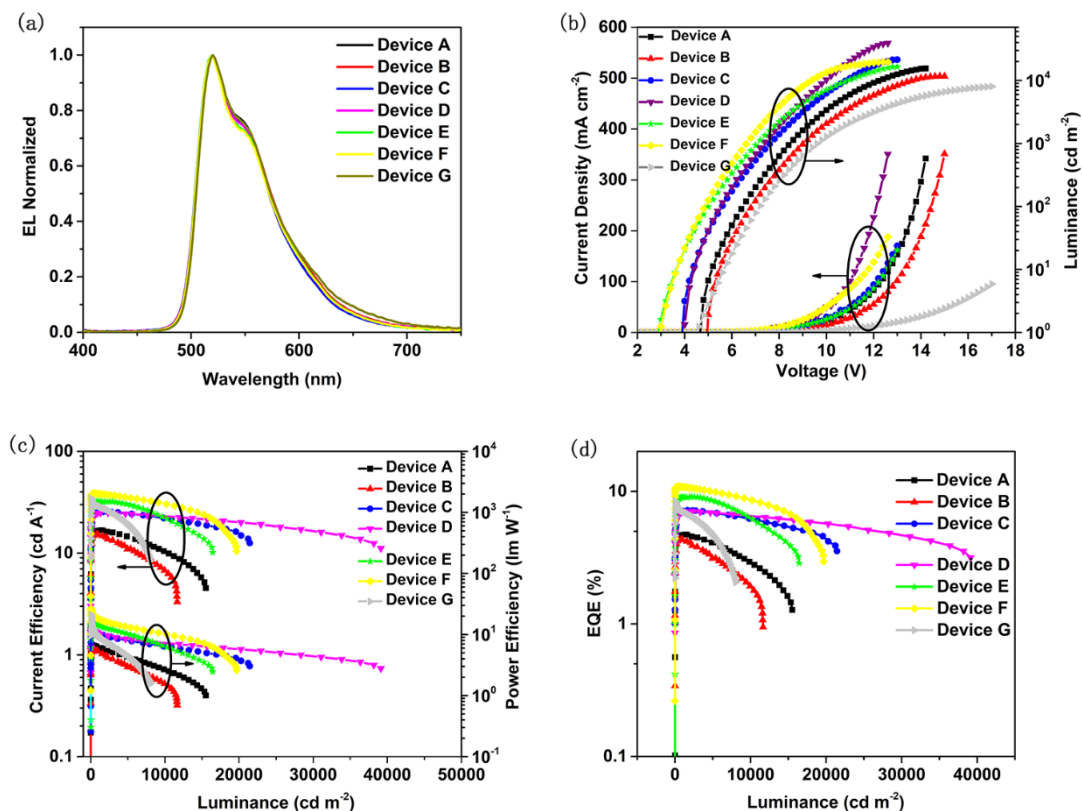


Figure 6. Green electrophosphorescence properties of Device A-G. (a) EL spectra. (b) J-V-L curves. (c) CE-L-PE curves. (d) EQE-L curves.

Table 2. Key parameters of Device A-G.

Devices	L_{\max} (cd m^{-2})	CE^a (cd A^{-1})	PE^a (lm W^{-1})	EQE^a (%)	V_{on} (V)	CIE
Device A	15521	16.80/13.10/16.68/14.51	6.67/6.31/6.19/4.12	4.73/3.61/4.74/4.02	4.8	(0.33,0.62)
Device B	11663	15.24/12.41/15.22/10.93	5.99/5.72/5.31/3.02	4.34/3.51/4.32/3.09	5.0	(0.33,0.62)
Device C	21441	25.50/18.84/25.30/14.32	11.37/10.61/10.43/7.79	7.20/5.33/7.12/6.93	4.0	(0.33,0.61)
Device D	39132	25.00/20.74/24.71/24.22	11.95/11.70/10.32/8.34	7.08/5.89/6.92/6.90	4.0	(0.34,0.61)
Device E	16436	32.18/25.43/31.96/30.33	16.21/16.01/14.00/10.32	9.09/7.21/9.01/8.55	2.9	(0.33,0.62)
Device F	19674	38.43/37.73/38.34/35.19	26.64/24.59/18.23/13.62	10.87/10.70/10.79/10.13	2.9	(0.33,0.62)
Device G	8037	34.75/32.30/29.18/19.35	21.14/14.135/9.55/4.45	8.48/7.89/7.12/4.69	4.6	(0.32,0.63)

^a: order of measured efficiency values: maximum, measured at 100 cd m^{-2} , measured at 1000 cd m^{-2} , measured at 5000 cd m^{-2} .

Conclusion

In summary, two alcohol-soluble electron transport materials (PBIPO) were designed and synthesized and their physical properties were investigated. The two ETMs exhibited deep LUMO levels of -2.87 eV and -2.82 eV, high T_1 of 2.63 eV and 2.67 eV, high electron transport mobility of $1.67 \times 10^{-4} \text{ cm}^2 \text{ V}^{-1} \text{ s}^{-1}$ and $2.15 \times 10^{-4} \text{ cm}^2 \text{ V}^{-1} \text{ s}^{-1}$, respectively. Green PhOLEDs utilizing PBIPO as ETMs were fabricated. For devices using mBPBIPO as ETMs, high efficiencies (CE, PE, EQE) of 38.43 cd A^{-1} , 26.64 lm W^{-1} , 10.87% and low V_{on} of 2.9 V were obtained. Compared with devices without PBIPO as ETMs, efficiencies of these devices were significantly increased, indicating that PBIPO was an excellent alcohol-soluble ETM.

Experimental Section

Materials

THF was freshly distilled from sodium/benzophenone under argon (Ar) atmosphere before use. Other reagents and solvents used for the synthesis and measurement were purchased from commercial suppliers without further purification.

General Procedures

^1H NMR spectrum were obtained on a Bruker ACF400 (400 MHz) spectrometer with tetramethylsilane as reference. The mass spectra data were obtained on micrOTOF-QII. Ultraviolet-visible absorption (UV-Vis) and photoluminescence (PL) spectra were measured on a Thermo Evolution 300 UV-Visible spectrometer and a HitachiF-4500 fluorescence spectrometer, respectively. The phosphorescence spectra was measured on Spectrofluorometer F7000. TGA was recorded on a TA Q500 at a heating rate of $10 \text{ }^\circ\text{C min}^{-1}$ under nitrogen atmosphere. DSC measurement was recorded on a TA Q20 instrument operated at a heating rate of $10 \text{ }^\circ\text{C min}^{-1}$ under N_2 atmosphere. Cyclic voltammetry was performed using a CHI600E analyzer at a scan rate of 100 mV s^{-1} . XRD spectra was recorded on MiniFlex 600. AFM was measured using NTEGRA Spectra. Photoluminescence quantum efficiency was measured on IS080 LabSphere integrating sphere.

OLED device fabrication and measurement

Indium tin oxide (ITO) glass substrates with sheet resistance of 30Ω per square were firstly pre-cleaned with isopropanol, acetone, detergent, diluted water and isopropanol under succession for 15 min, then dried in an oven, treated with UV-ozone for 2 min. An anode modified layer was obtained by spin-coating the PEDOT: PSS aqueous solution on ITO substrates at 3000 rpm, followed with annealing at 150°C for 20 min. The 10 mg mL^{-1} concentrated PVK was spin-coated on the PEDOT: PSS layer and PVK layer was obtained by annealing at 150°C for 20 min. Then ITO was transferred to the glove box and 10 mg mL^{-1} concentrated host2: IrG1=95:5 was spin-coated on the PVK layer. A 65nm thick emitting layer was obtained by annealing at 120°C for 20 min. The 10 mg mL^{-1} concentrated PBiPO n-butyl alcohol solution was spin-coated on the emitter layer. The ITO substrate above was transferred into the deposition chamber. Then 0.8 nm CsF was deposited at a rate of 0.1 \AA s^{-1} and 100 nm Al was deposited at a rate of 1 \AA s^{-1} under the vacuum of 2×10^{-6} Pa. For all devices, the light-emitting areas were determined as 0.16 cm^2 . The EL spectra, luminance of device, and CIE coordinates were measured with Ocean Optics USB2000+. The current-voltage-luminance characteristics were measured by Keithley 2400 source meter and Konica Minolta Chroma Meter CS-200 with silicon photodiode under ambient atmosphere with device encapsulation. The thicknesses of the spin-coated films were measured by the Dektak 150 surface profiler terrace detector.

Synthesis and characterizations

The pBiPO was synthesized according to the reported procedure^[15] and synthesis routes of mBiPO are as follows:

(1) Synthesis of 5-bromoisophthaloyl dichloride (compound 3)

Oxalyl chloride was added dropwise to a mixture of 5-bromoisophthalic acid (1.23 g, 5.0 mmol), $20 \text{ mL CH}_2\text{Cl}_2$ and DMF (two drops) under N_2 at room temperature and then refluxing. After 12 hours, removing the solvent by vacuum distillation to afford the yellow oil liquid.

(2) Synthesis of 2,2'-(5-bromo-1,3-phenylene)bis(1-phenyl-1*H*-benzo[*d*]imidazole) (compound 4)

Compound 3 (5-Bromoisophthaloyl dichloride) was added dropwise to a mixture of N-phenyl-1,2-*o*-phenylenediamine (2.03 g, 11 mmol), triethylamine (2.5 mL) and NMP (20 mL) under Ar at room temperature and then heated to 160°C . After 24

hours, it was poured into water and extracted with CH_2Cl_2 . The solvent was removed and the crude product was recrystallized in CH_2Cl_2 and methanol to afford a grey solid of compound 4. Yield: 1.08 g, 40.0%. ^1H NMR (400 MHz, DMSO) δ 7.81 (d, J = 7.4 Hz, 2H), 7.75 (s, 1H), 7.63 (dd, J = 13.0, 4.4 Hz, 6H), 7.58 – 7.52 (m, 2H), 7.42 – 7.27 (m, 8H), 7.20 (d, J = 7.4 Hz, 2H).

(3) Synthesis of mBPBIPO

A mixture of compound 4 (0.540 g, 1.0 mmol), diphenylphosphine oxide (0.202 g, 1.0 mmol), Zn (0.131 g, 2.0 mmol), 2, 2'-bipyridine (0.0310 g, 0.20 mmol), $\text{NiCl}_2 \cdot 6\text{H}_2\text{O}$ (0.0238 g, 0.10 mmol) and DMAC (20 mL) was stirred under N_2 at 150 °C for 24 hours. After cooling to room temperature, it was poured into water and extracted with CH_2Cl_2 . The organic layer was dried with MgSO_4 and filtered. The crude product was isolated by silica gel column chromatography using methanol / CH_2Cl_2 as eluent to afford a white solid. Yield: 0.300 g, 45.2%. ^1H NMR (400 MHz, DMSO) δ = 8.32 (s, 1H), 7.80 (d, J = 7.7 Hz, 2H), 7.67 – 7.60 (m, 3H), 7.59 (d, J = 1.1 Hz, 1H), 7.55 (s, 1H), 7.52 (dd, J = 13.7, 5.1 Hz, 7H), 7.48 – 7.42 (m, 2H), 7.31 (dd, J = 17.3, 6.6 Hz, 9H), 7.26 (d, J = 4.4 Hz, 2H), 7.23 (s, 1H), 7.18 (d, J = 7.7 Hz, 2H); ^{13}C NMR (101 MHz, CDCl_3) δ = 150.63, 142.93, 137.12, 136.18, 134.38, 133.91, 133.13, 133.03, 132.90, 131.99, 131.94, 131.92, 131.89, 131.84, 131.37, 131.24, 130.94, 129.94, 128.74, 128.60, 128.47, 127.23, 123.81, 123.23, 120.18, 110.58. HRMS calcd for $\text{C}_{44}\text{H}_{31}\text{N}_4\text{OP}$: 662.73; found, 663.2, ($m+1$), 685.2, ($M+23$).

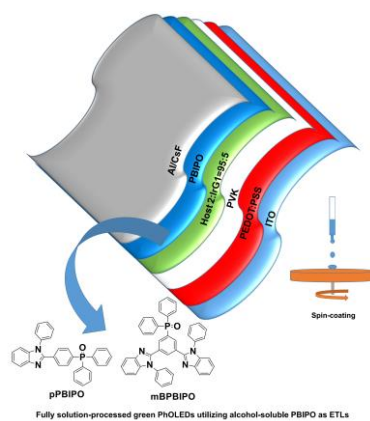
Acknowledgements

This work was supported by the National Key Research and Development Program of China (2016YFB0401303).

Key words: alcohol-soluble • electron transport material • fully solution-processed • PhOLED

- [1] (a) C. W. Tang, S. A. Vanslyke, *Appl. Phys. Lett.* **1987**, 51 (12), 913-915; (b) J. Kido, M. Kimura, K. Nagai, *Science*. **1995**, 267 (5202), 1332-4; (c) B. W. D'Andrade, S. R. Forrest, *Adv. Mater.* **2004**, 16.
- [2] (a) R. Liu, X. Xu, J. Peng, C. Yao, J. Wang, L. Li, *Rsc Adv.* **2015**, 5 (46), 36568-36574; (b) W. Jiang, H. Xu, X. Ban, G. Yuan, Y. Sun, B. Huang, L. Duan, Y. Qiu, *Org. Lett.* **2014**, 16 (4), 1140-3.
- [3] (a) N. Aizawa, Y. J. Pu, M. Watanabe, T. Chiba, K. Ideta, N. Toyota, M. Igarashi, Y. Suzuri, H. Sasabe, J. Kido, *Nature Commun.* **2014**, 5, 5756; (b) K. S. Yook, S. E. Jeon, S. O. Jeon, J. Y. Lee, *Adv. Mater.* **2010**, 22 (40), 4479-83.

- [4] (a) X. Ban, K. Sun, Y. Sun, B. Huang, W. Jiang, *Org. Electron.* **2016**, 33, 9-14; (b) S. Ye, L. I. Le, M. Zhang, M. Quan, Z. Zhou, L. Guo, Y. Wang, M. Yang, W. Y. Lai, W. Huang, *J. Mater. Chem. C.* **2017**; (c) A. Lorente, P. Pingel, A. Miasojedovas, H. Krueger, S. Janietz, *Acs Appl Mater Interfaces.* **2017**, 9 (28); (d) W. Jiang, J. Tang, X. Ban, Y. Sun, L. Duan, Y. Qiu, *Org. Lett.* **2014**, 16 (20), 5346-9.
- [5] (a) H. J. Bolink, E. Coronado, S. S. Garcia, M. Sessolo, N. Evans, C. Klein, E. Baranoff, K. Kalyanasundaram, M. Graetzel, M. K. Nazeeruddin, *Chem. Commun.* **2007**, 31 (31), 3276-3278; (b) M. Lepeltier, F. Dumur, G. Wantz, N. Vila, I. Mbomekallé, D. Bertin, D. Gigmes, C. R. Mayer, *J. Lumin.* **2013**, 143 (6), 145-149; (c) Y. Fang, B. Tong, S. Hu, S. Wang, Y. Meng, J. Peng, B. Wang, *Org. Electron.* **2009**, 10 (4), 618-622; (d) G. Ge, G. Zhang, H. Guo, Y. Chuai, D. Zou, *Inorg. Chim. Acta.* **2012**, 362 (7), 2231-2236; (e) R. J. Holmes, S. R. Forrest, T. Sajoto, A. Tamayo, *Appl. Phys. Lett.* **2005**, 87 (24), 243507-243507-3.
- [6] (a) F. Huang, L. Hou, H. Wu, X. Wang, H. Shen, W. Cao, W. Yang, Y. Cao, *J. Am. Chem. Soc.* **2004**, 126 (31), 9845-53; (b) F. Huang, H. Wu, Y. Cao, *Chem. Soc. Rev.* **2010**, 39 (7), 2500-21.
- [7] (a) P. Stroehriegel, J. V. Grazulevicius, *Adv. Mater.* **2002**, 14 (20), 1439-1452; (b) S. Sax, N. Rugen-Penkalla, A. Neuhold, S. Schuh, E. Zojer, E. J. W. List, K. Müllen, *Adv. Mater.* **2010**, 22 (18), 2087-2091; (c) S. Sax, G. Mauthner, T. Piok, S. Pradhan, U. Scherf, E. J. W. List, *Org. Electron.* **2007**, 8 (6), 791-795.
- [8] X. He, L. Chen, Y. Zhao, S. Ng, X. Wang, X. Sun, X. MatthewHu, *Rsc Adv.* **2015**, 5 (20), 15399-15406.
- [9] (a) S. O. Jeon, K. S. Yook, C. W. Joo, J. Y. Lee, *J. Mater. Chem.* **2009**, 19 (33), 5940-5944; (b) P. E. Burrows, A. B. Padmaperuma, L. S. Sapochak, P. Djurovich, M. E. Thompson, *Appl. Phys. Lett.* **2006**, 88 (18), 2082-9.
- [10] A. P. Kulkarni, C. J. Tonzola, A. Amit Babel, S. A. Jenekhe, *Chem. Mater.* **2004**, 16 (23), 4556-4573.
- [11] T. D. Anthopoulos, J. P. J. Markham, E. B. Namdas, I. D. W. Samuel, S. C. Lo, P. L. Burn, *Appl. Phys. Lett.* **2003**, 82 (26), 4824-4826.
- [12] Z. Gao, C. S. Lee, I. Bello, S. T. Lee, R. M. Chen, T. Y. Luh, J. Shi, C. W. Tang, *Appl. Phys. Lett.* **1999**, 74 (6), 865-867.
- [13] Z. Ge, T. Hayakawa, S. Ando, M. Ueda, T. Akiike, H. Miyamoto, T. Kajita, M. A. Kakimoto, *Adv. Funct. Mater.* **2008**, 18 (4), 584-590.
- [14] F. A. Alasmay, A. M. Snelling, M. E. Zain, A. M. Alafeefy, A. S. Awaad, N. Karodia, *Molecules.* **2015**, 20 (8), 15206-23.
- [15] B. Wang, X. Lv, B. Pan, J. Tan, J. Jin, L. Wang, *J. Mater. Chem. C.* **2015**, 3 (42), 11192-11201.
- [16] S. J. Su, T. Chiba, T. Takeda, J. Kido, *Adv. Mater.* **2008**, 20 (11), 2125-2130.
- [17] E. Ahmed, T. Earmme, S. A. Jenekhe, *Adv. Funct. Mater.* **2011**, 21 (20), 3889-3899.
- [18] N. Zhou, S. Wang, Y. Xiao, X. Li, *Chem – Asian J.* **2017**.
- [19] M. Cekaviciute, J. Simokaitiene, D. Volyniuk, G. Sini, J. V. Grazulevicius, *Dyes Pigm.* **2017**, 140, 187-202.
- [20] X. Zhao, S. Wang, J. You, Y. Zhang, X. Li, *J. Mater. Chem. C.* **2015**, 3 (43).
- [21] W. Sun, N. Zhou, Y. Xiao, S. Wang, X. Li, *Chem – Asian J.* **2017**, 12 (23), 3069.
- [22] (a) T.-Y. Chu, O.-K. Song, *Appl. Phys. Lett.* **2007**, 90 (20), 151; (b) M. A. Khan, W. Xu, Khizar-ul-Haq, Y. Bai, X. Y. Jiang, Z. L. Zhang, W. Q. Zhu, Z. L. Zhang, W. Q. Zhu, *J. Appl. Phys.* **2008**, 103 (1), 913.
- [23] W. S. Jeon, O. Hyoung-Yun, J. S. Park, J. H. Kwon, *Mol. Cryst. Liq. Cryst.* **2011**, 550 (1), 311-319.
- [24] N. Aizawa, Y. J. Pu, T. Chiba, S. Kawata, H. Sasabe, J. Kido, *Adv. Mater.* **2014**, 26 (45), 7543-6.
- [25] N. Zhou, X. Shao, S. Wang, Y. Xiao, X. Li, *Org. Electron.* **2017**, 50.



Fully solution-processed green PhOLEDs utilizing alcohol-soluble PBiPO as ETMs.